Electronic Supplementary Material (ESI) for Dalton Transactions.

Electronic Supplementary Information (ESI) for

The role of titanium-oxo clusters in sulfate production of TiO_2

Karoly Kozma [a], Maoyu Wang [b], Pedro I. Molina [a,c], Nicolas P. Martin[a], Zhenxing Feng [b], May Nyman *[a]

[a] Department of Chemistry, Oregon State University, 153 Gilbert Hall, Corvallis, OR 97331, USA
[b] School of Chemical, Biological and Environmental Engineering, Oregon State University, Corvallis, OR 97331, USA
[c] current address: Valliscor, Advanced Technology & Manufacturing Institute, 111 NE Circle Blvd, Corvallis, OR 97330, USA
*Corresponding author. E-mail address: May.Nyman@oregonstate.edu

This file includes:

Supplementary text
Figures S1 to S12
Tables S1 to S4
References for ESI reference citations

Supplementary Information Text

Characterization methods

1. Small-angle X-ray scattering (SAXS)

Small-angle X-ray scattering data were collected on Anton Paar SAXSess instrument using Cu-Kα radiation (λ=1.54056 Å), line collimation, 2D image plates and the range of momentum transfer (*q*) of 0.018-2.5 $Å^{-1}$. All solutions, including background solutions, were contained in sealed borosilicate tubes of 1.5 mm in diameter and 0.01 mm wall thickness (HR6-124, Hampton Research) placed at a distance of 26.1 cm from the image plates. Data collection time of 30 minutes was utilized.

We used SAXSQUANT software for data collection and treatment including normalization, primary beam removal, background subtraction, desmearing and smoothing. Analyzes, fits were carried out utilizing IRENA macros with IgorPro 6.3 (Wavemetrics) software[1]. To simulate scattering data from the crystal structure we used SolX software[2,3].

2. Extended X-ray absorption fine structure (EXAFS)

EXAFS measurements were done at 9BM and 20BM of Advanced Photon Source of Argonne National Laboratory. The solution is filled in a custom-designed holder that has a small window covered by Kapton film. The X-ray can penetrate the Kapton film without too much attenuation. The florescence mode is used to collect Ti K-edge signal.

To perform EXAFS, 0.2 mL solution filtered through a syringe is filled in a custom-designed holder that has a 20 × 5 mm^2 Kapton window. All data were collected in a fluorescence mode. A Vortex ME4 detector was used to collect the Ti K fluorescence signal while a Si(111) monochromator scanned the incident X-ray photon energy through the Ti K absorption edge. The monochromator was detuned to 65% of the maximum intensity at the Ti K edge to minimize the presence of higher harmonics. At least four scans for each sample were carried out to ensoure data statistics for XAS. The X-ray beam was calibrated using a Ti metal foil. Data reduction, data analysis, and EXAFS fitting were performed with the Athena, Artemis, and IFEFFIT software packages. Standard procedures were used to extract the EXAFS data from the measured absorption spectra. The pre-edge background was linearly fitted and subtracted. The post-edge background was determined using a spline-interpolation procedure and then subtracted. Normalization was performed by dividing the data by the height of the absorption edge at 50 eV. For quantitative analysis, phase shifts and back-scattering amplitudes were generated by the FEFF calculations based on crystal structures of TiO_2 and $\{Ti_{18}\}$, and were then calibrated through performing the FEFFIT of the EXAFS data of the reference samples, mainly to obtain the amplitude reduction factor (S_0^2) values. With S_0^2 known, the EXAFS data of the materials were fitted with such generated phase shifts and amplitudes.

3. Pair distribution function analysis (PDF) of X-ray total scattering measurements

To perform pair distribution function (PDF) analysis we used Rigaku Smartlab X-ray diffractometer with Mo-Kα irradiation (λ=0.71 Å) in the 2θ range of 3-118.0° with transmission geometry. The theoretical *q*-range is up to a q_{max} of 15.4 $Å^{-1}$. A 0.2 degree/minute data collection time was used to ensure high quality scattering data. Samples were loaded in Kapton capillary with 1.46 mm inner diameter for irradiation.

PDFgetX3 was to process scattering data into the corresponding PDF[4]. Simulations were created in PDFgui[5].

4. Transmission Electron Microscopy (TEM)

Images were acquired using a high angle annual dark field detector on an FEI Titan TEM operated at 200 keV in STEM mode. Specimens were supported on holey carbon grid. The specimens were prepared by micro-pipetting a droplet of solution on a TEM grid and allowing it to dry completely in air.

5. Energy-Dispersive X-ray Spectroscopy (EDX)

Energy dispersive X-ray spectroscopy (EDX) measurements were performed on Quanta 600 scanning electron microscopy (SEM) to extract composition information of the precipitated solid sample.

6. Crystallography

Single crystal X-ray diffraction data on the obtained crystals were collected on a Bruker DUO-APEX2 CCD area-detector diffractometer at 173 K using Cu-Kα (1.54178 Å) radiation. Data reduction was accomplished using SAINT V8.34a[6]. The substantial redundancy in data allowed a semiempirical absorption correction[7] to be applied, based on multiple measurements of equivalent reflections. The structures were solved by the intrinsic phasing method from the SHELXT program[8], developed by successive difference Fourier syntheses, and refined by full-matrix least squares on all F^2 data using SHELX[9] via OLEX2[10] interface. The crystal data is given in **Table S2**. CCDC files number: 1898206 contains the supplementary crystallographic data for this paper. These data can be obtained, free of charge, from The Cambridge Crystallographic Data Centre via www.ccdc.cam.ac.uk/structures

Details about structural refinement and sulfate-Cl disorder for crystallized {Ti_{18}}

We had significant difficulties obtaining the precise crystal structure of the investigated compound. Several data collections with different crystals were made. All crystals tested for single-crystal X-ray diffraction are twinned, consisting of two plates joined together with opposite orientations. Standard integrations of the data as for two component twin in all cases were failed; such integrations did not improve the quality of the model outside the main **{Ti_{18}}**-cluster core. Therefore, a twin law (-1 0 0; 0 -1 0; 0 0 1) found based on Cell_now was applied during the refinement process (BASF 0.09 and flack 0.11). Furthermore, all crystals were weakly diffracting due to a strong disorder for counter-ions and solvent molecules outside the main Ti_{18}-cluster. Even using a strong Incoatec Cu IμS source it was possible to collect data only up to 2θ max = 100 degrees (**Figure S7**). This is mainly due to the presence of highly disordered solvent molecules. However, with these limitations, the data provided an appropriate number of measured reflections per refined parameters, 19697/2207 and allowed to prove we crystallized the {Ti_{18}} cluster.

However, the **{Ti_{18}}**-cluster in the structure is suitably determined. As presented prior, three layers of $Ti(Ti)_5$ form the Ti_{18} cluster and we were able to localize eight fully occupied sulfate positions. Seven of these are located on the outside layers, each bridging two Ti^{4+}. The eighth fully occupied sulfate is terminally bound to a Ti on one of the outside layers. There is an additional sulfate that is half-occupied, also terminally bound on the outside layer. One of the oxos of this sulfate is disordered with a Cl^-, ~3.0 Å from a Ti-bound water (**Figure S9**). The second disordered sulfate is actually three sites; two are terminally bound to the outside layer on adjacent Ti's (illustrated in **Figure S8**). The third sulfate is free from the cluster, but also mutually shares an oxo position with one of the other disordered sulfates. To determine the occupancies, these three sulfur sites were first freely refined, which gave values close to 1/3rd for each. Therefore we fixed each of these at 0.333 occupancy, for a total of one sulfate. The sum total of sulfates based on this model is 9.5 per **{Ti$_{18}$}**. The aforementioned half-occupied, cluster-bound sulfate likewise has one oxo ligand disordered with chloride. This mixed oxo-Cl site freely refined close to ½S-½O, in agreement with occupancy of the sulfur. Finally, we located 4 fully occupied Cl in the electron density map, and one ½-occupied Cl for a total of 5.5 Cl. The chlorides are mostly frequently located ~3 Å from terminal water ligands of the cluster, likely serving a role in stabilizing the cluster for crystal growth via non-covalent interactions. Six TBA molecules were fully located in the electron density map but also highly disordered, especially for the terminal groups. Crystallographic details about structure refinement for the obtained structure is collected in **Table S2,** and further detailed in the ESI.

Figures and tables

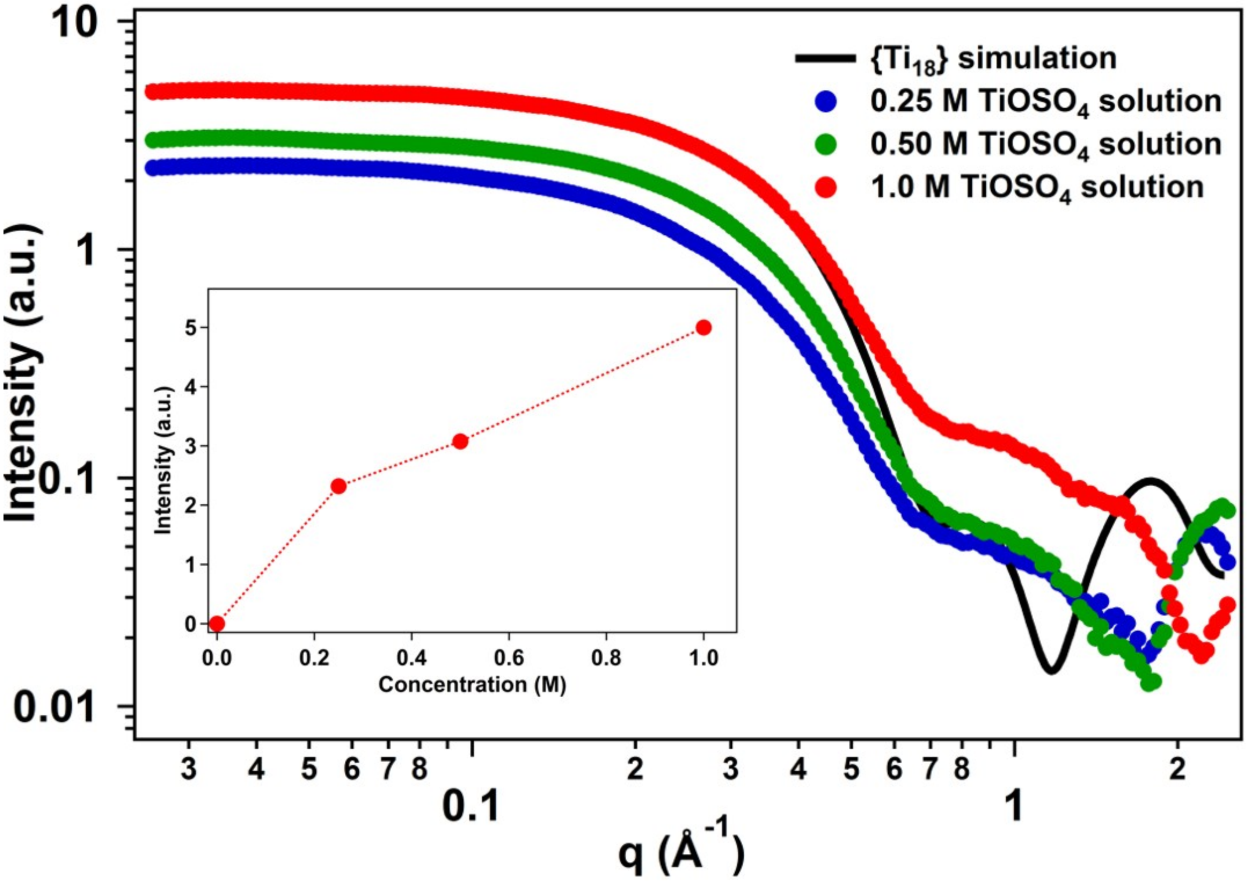

Figure S1 SAXS curves of dissolved $TiOSO_4$ in water (blue: 0.25M, green: 0.5M and red: 1.0M concentration). Inset shows the relation between the concentration at the observed intensity at q=0.3 Å^{-1}.

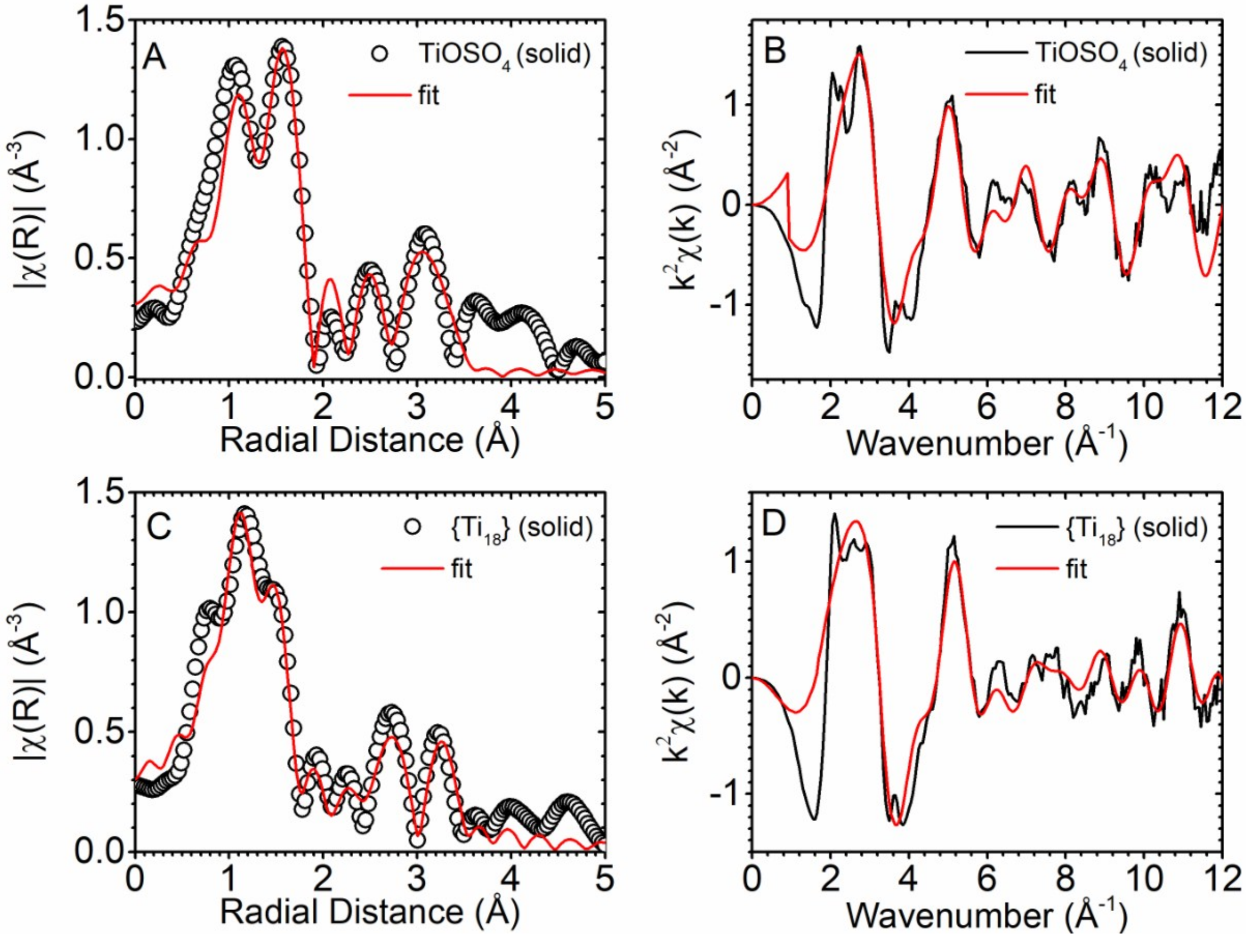

Figure S2 Ti K-edge EXAFS Fourier Transformation R-space modeling based fitting of (A) $TiOSO_4$ powder and (C) $\{Ti_{18}\}$ powder; K-space of (B) $TiOSO_4$ powder and (D) $\{Ti_{18}\}$ powder

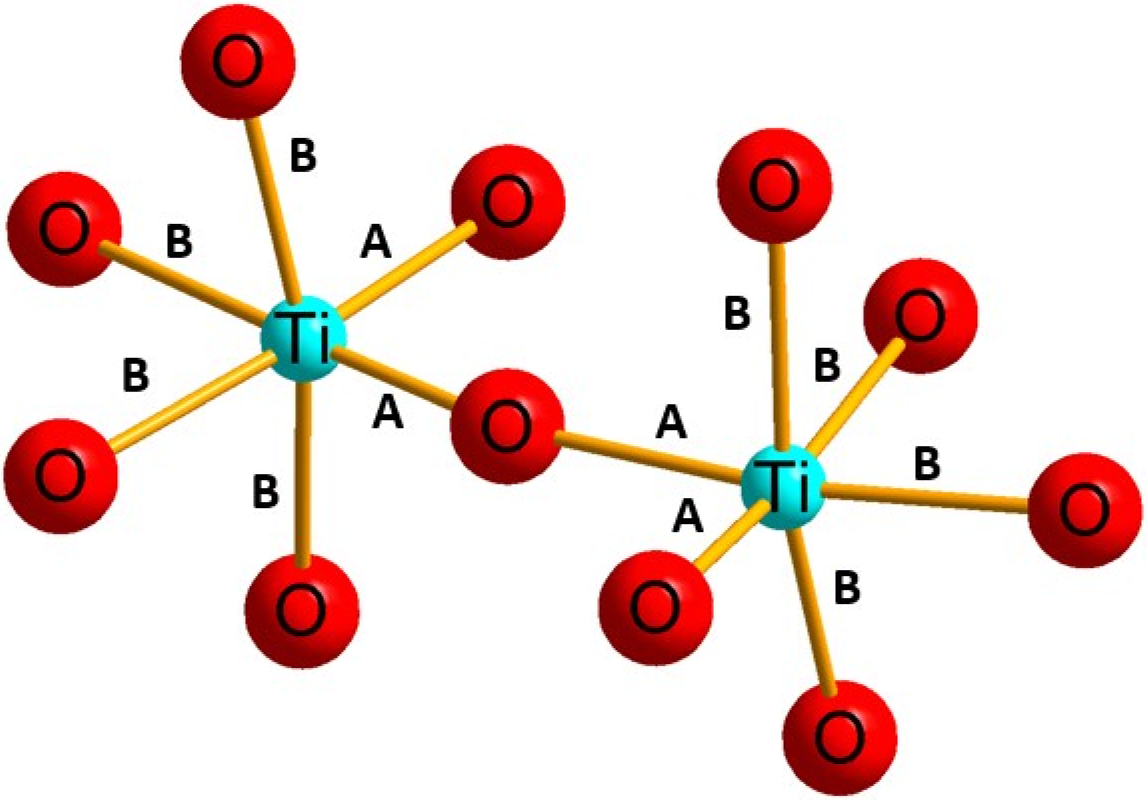

Figure S3 The observed Ti-O distances in Ti-O polyhedra in the $TiOSO_4 \cdot H_2O$ unit cell (ICSD: 72973). Sulfate groups are eliminated for clarification. Letters represents the observed Ti K-edge EXAFS correlations assigned in **Table S1**.

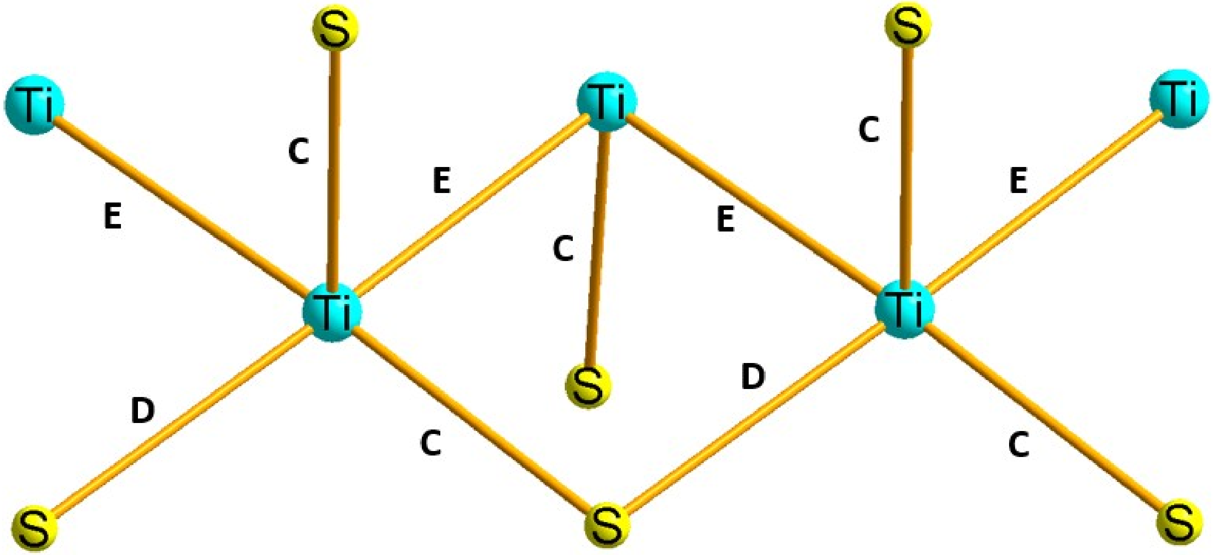

Figure S4 The observed Ti-Ti and Ti-S correlations in $TiOSO_4 \cdot H_2O$ crystal structure (ICSD: 72973) Oxygens and hydrogens are eliminated for clarification. Letters represents the observed Ti K-edge EXAFS correlations assigned in **Table S1**.

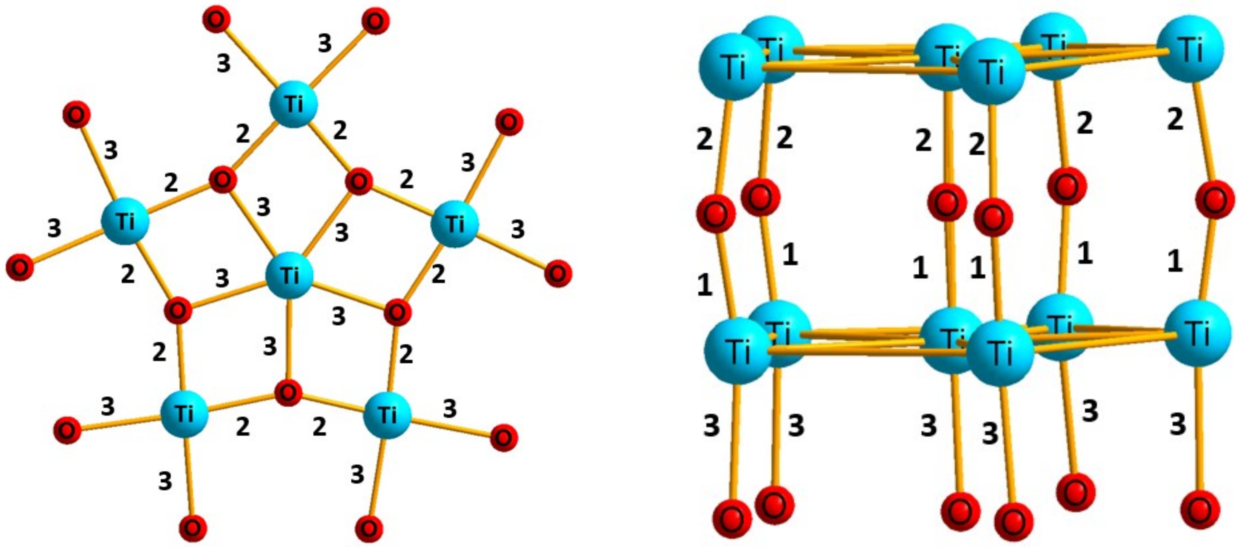

Figure S5 The observed equatorial Ti-O correlations in a pentagonal Ti(Ti)$_5$ unit (left) and the horizontal Ti-O correlations between two Ti(Ti)$_5$ layers in {Ti$_{18}$}-cluster (right). Sulfur, oxygen and hydrogen atoms are eliminated for clarification. Numbers represents the observed Ti K-edge EXAFS correlations assigned in **Table S1**.

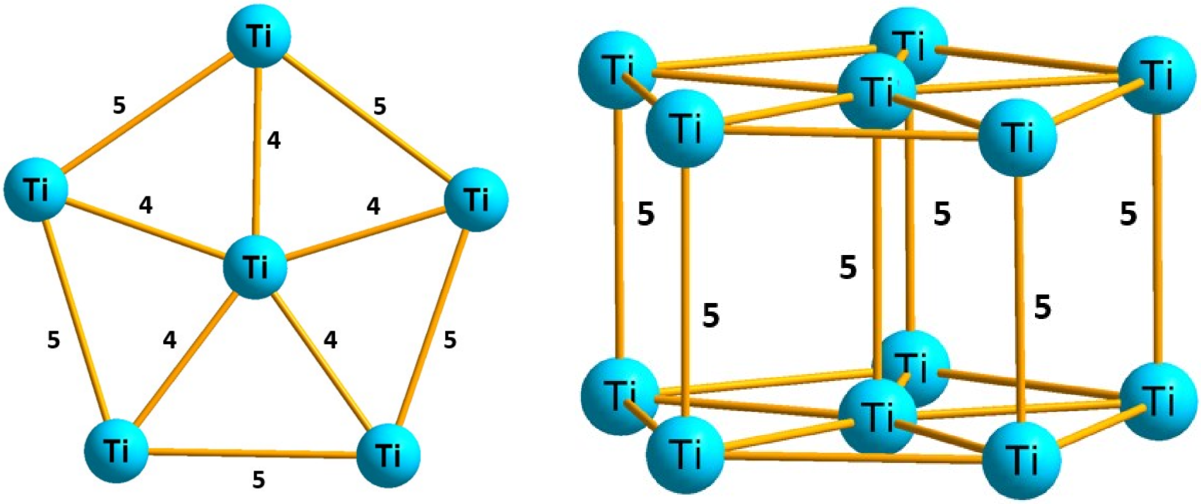

Figure S6 The observed Ti-Ti correlations in one pentagonal Ti(Ti)$_5$ unit (left) and between two layers of Ti(Ti)$_5$ unit in the {Ti$_{18}$}-cluster (right). Sulfur, oxygen and hydrogen atoms are eliminated for clarification. Numbers represents the observed Ti K-edge EXAFS correlations assigned in **Table S1**.

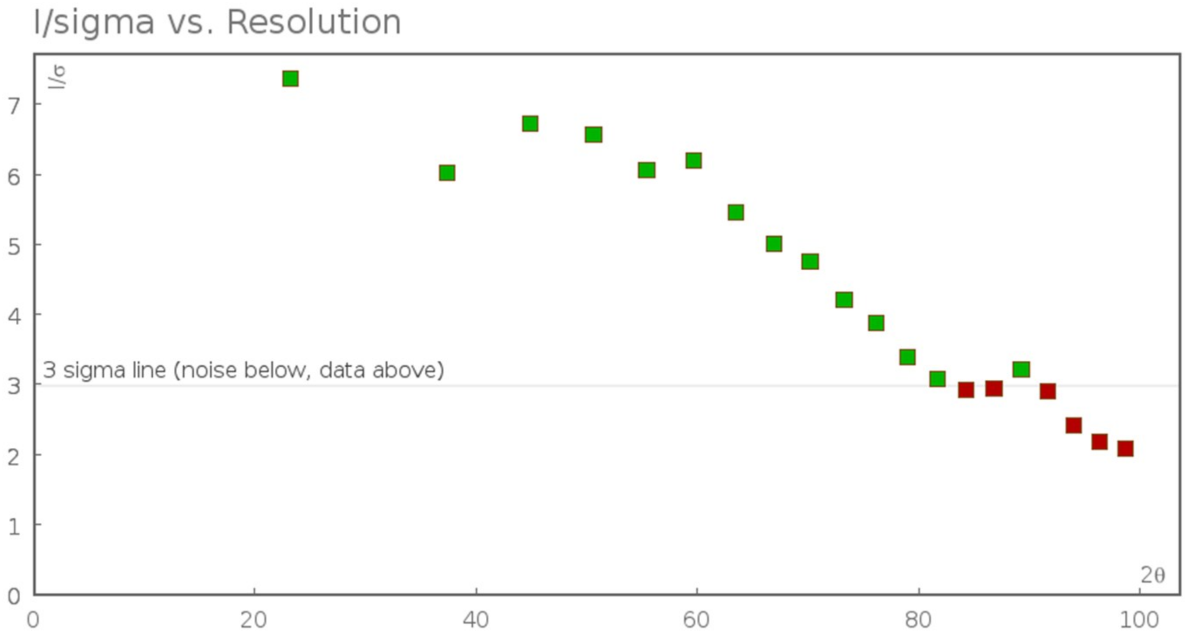

Figure S7 Representation of the average intensity according to the 2theta angle for single crystal structure.

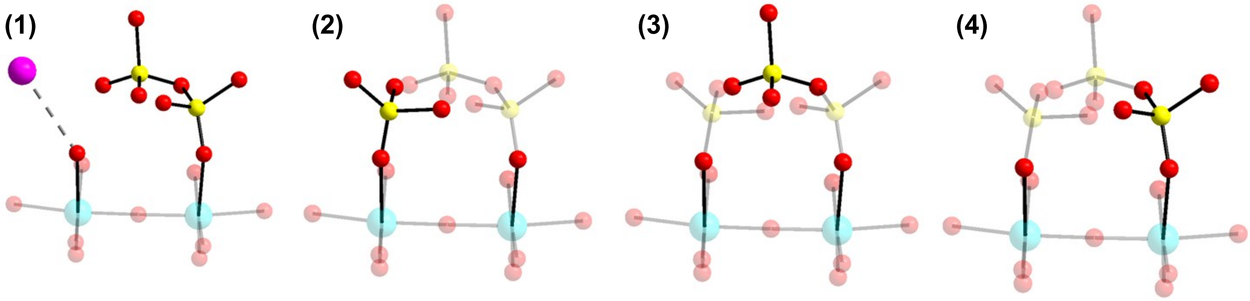

Figure S8 Illustration of disorder model between three sulfates and a Cl^- anion on one face of the $\{Ti_{18}\}$ cluster. The two Ti-centers of the cluster to which the disordered sulfates bind/associate are shown partially transparent (Ti is turquoise, O is red, S is yellow, Cl is pink). **(1)** half-occupied Cl^-, ~3 Å from the Ti-bound water ligand, present only when sulfate 3 or 4 is present. **(2)** sulfate-1; 1/3rd occupied; **(3)** sulfate-2; 1/3rd occupied; **(4)** sulfate-3; 1/3rd occupied. The sulfur atoms freely refined around 1/3rd occupancy, so we fixed the occupancy to 1/3rd; and likewise fixed the associated oxos appropriately. When a sulfate is not bound to the Ti, there is a water molecule (H's not show, nor located in the electron density map). Therefore Ti is always octahedrally-coordinating to six oxygen atoms.

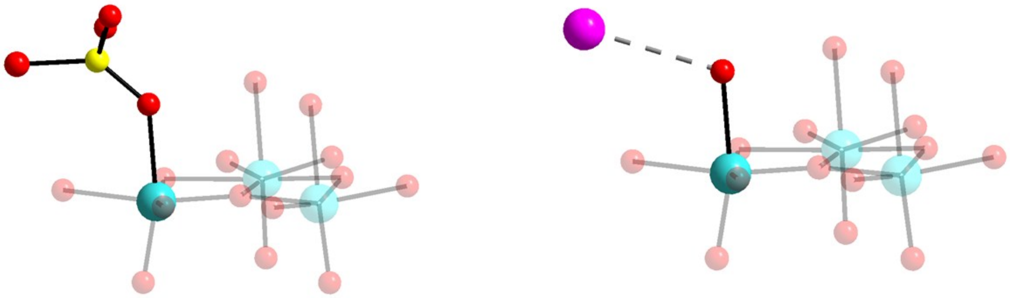

Figure S9 Illustration of sulfate-chloride disorder model on the opposite face of the cluster that is described in **Figure S8**. There are two settings (each 50% occupied) in this model. The first is with sulfate terminally bound to a Ti in the capping layer of Ti_{18}. The second is with a water molecule bound to the Ti; the Cl-atom is 3 Å from the oxygen of this water molecule. Color scheme is the same as described for **Figure S8**.

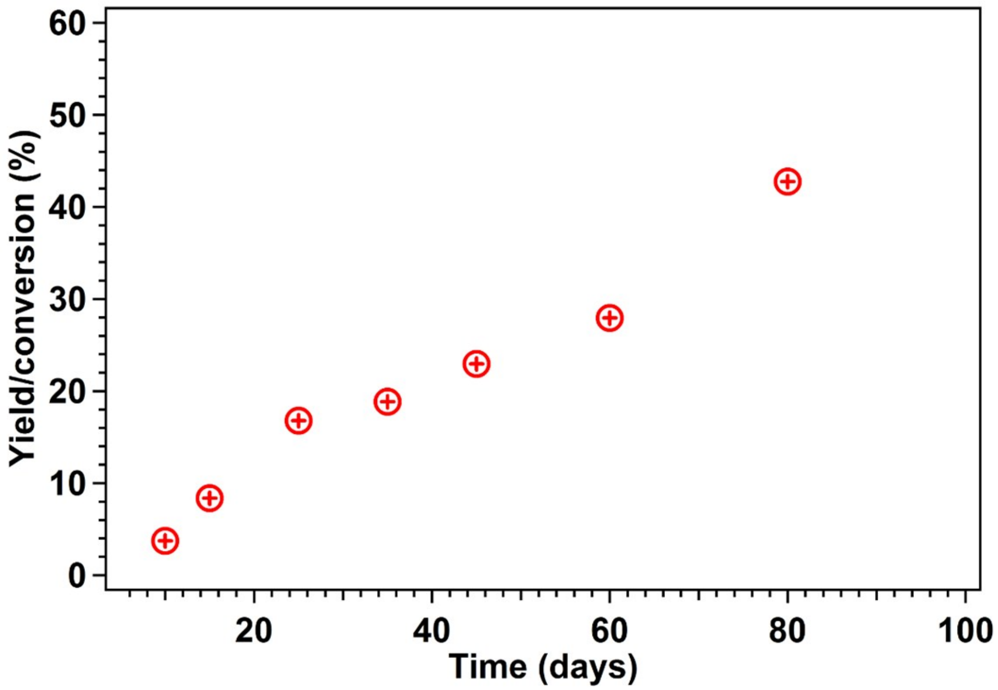

Figure S10 Calculated yield of anatase formation from 0.25M $TiOSO_4$ solution at ambient conditions.

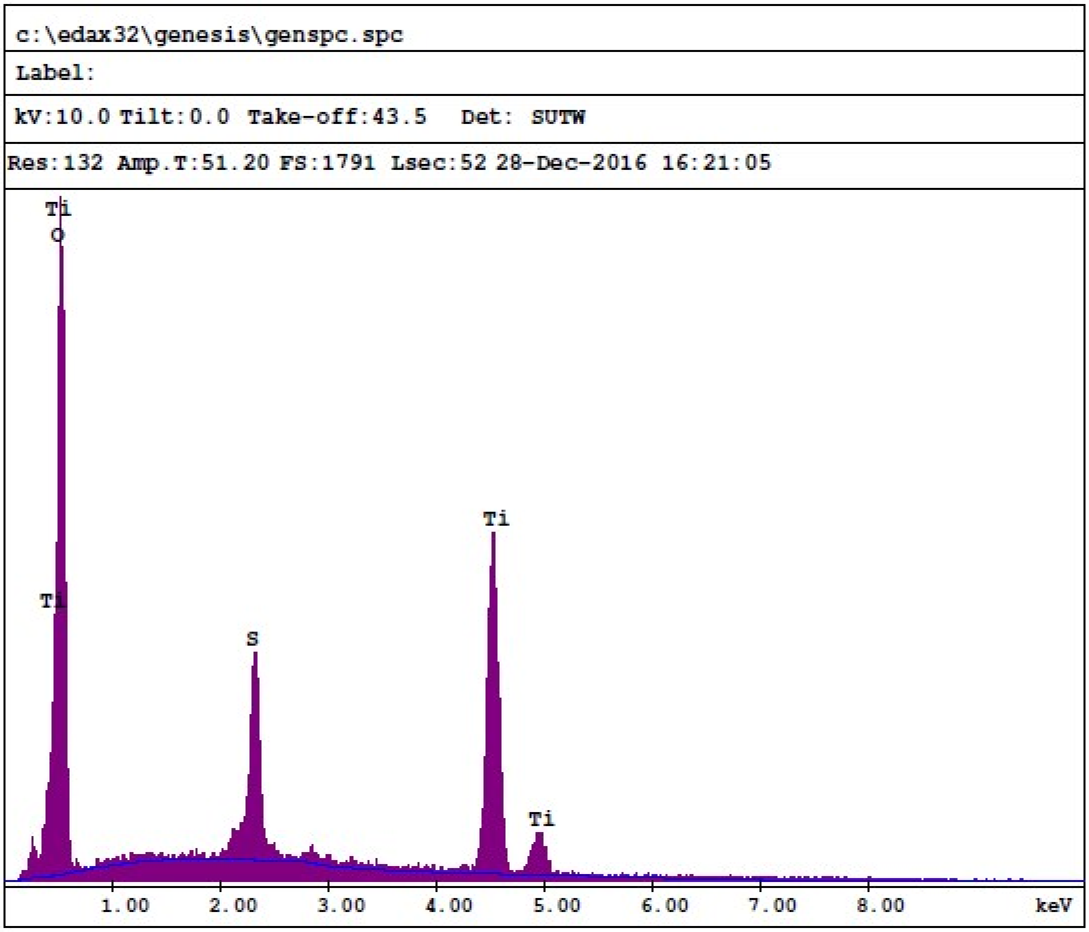

```
c:\edax32\genesis\genspc.spc
Label:
kV:10.0 Tilt:0.0 Take-off:43.5   Det: SUTW
Res:132 Amp.T:51.20 FS:1791 Lsec:52 28-Dec-2016 16:21:05
```

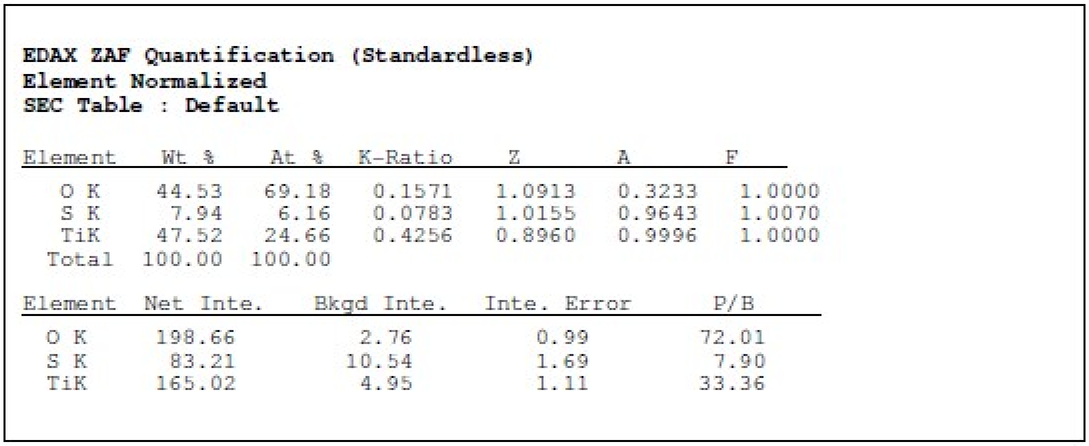

```
EDAX ZAF Quantification (Standardless)
Element Normalized
SEC Table : Default

Element    Wt %     At %   K-Ratio     Z         A         F
   O K    44.53    69.18   0.1571   1.0913    0.3233    1.0000
   S K     7.94     6.16   0.0783   1.0155    0.9643    1.0070
   TiK    47.52    24.66   0.4256   0.8960    0.9996    1.0000
  Total  100.00   100.00

Element   Net Inte.    Bkgd Inte.   Inte. Error      P/B
  O K      198.66         2.76          0.99        72.01
  S K       83.21        10.54          1.69         7.90
  TiK      165.02         4.95          1.11        33.36
```

Figure S11 EDX spectrum of the obtained precipitated solid from 0.25 M $TiOSO_4$ solution. The observed S:Ti ratio is 1:4.

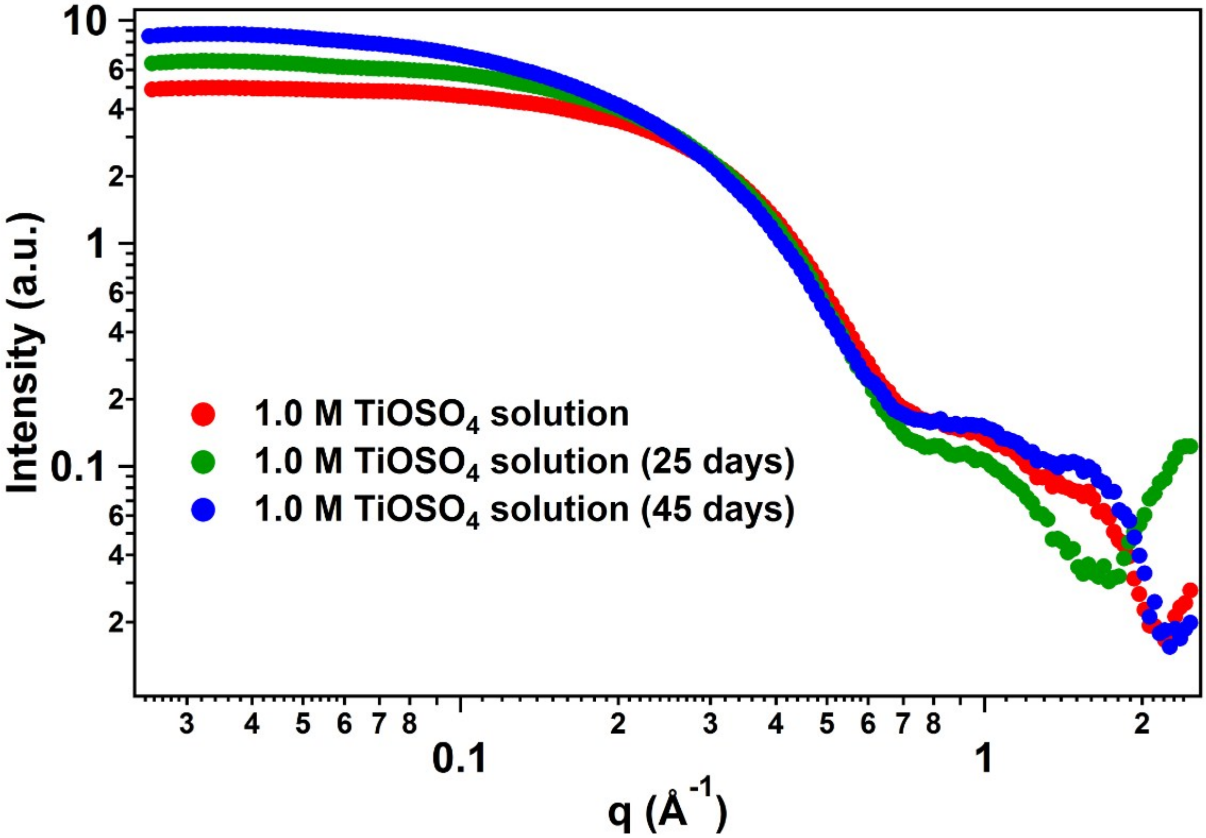

Figure S12 SAXS curves of aged samples of 1.0M $TiOSO_4$ solutions.

Table S1 EXAFS fitting parameters for $TiOSO_4$ and {Ti_{18}} in both solid phase and aqueous solution phase (CN: the coordination number; R: bonding distance; E_0: energy shift; σ^2: mean-square disorder)

	Scattering Path	**CN**	**R**	**E_0**	**σ^2**	**Notation**
$TiOSO_4$ solution						
	Ti-O	0.94±0.20	1.77±0.20	7.05±3.02	0.0007±0.0013	
	Ti-O	1.88±0.40	1.94±0.03	7.05±3.02	0.0113±0.0782	
	Ti-O	0.94±0.20	1.98±0.03	7.05±3.02	0.0039±0.0613	
	Ti-S / Ti-Ti	1.88±0.40	3.23±0.04	7.05±3.02	0.0013±0.0046	
	Ti-O-S	1.88±0.40	3.51±0.05	7.05±3.02	0.0077±0.0457	
	Ti-Ti	1.88±0.40	3.58±0.05	7.05±3.02	0.0094±0.0396	
	Ti-O-Ti	3.75±0.80	3.59±0.05	7.05±3.02	0.0054±0.0116	
	Ti-O-Ti	1.88±0.40	3.60±0.5	7.05±3.02	0.0080±0.0223	
{Ti_{18}} solution						
	Ti-O	0.61±0.17	1.78±0.13	8.71±2.48	0.0008±0.0012	
	Ti-O	0.61±0.17	1.88±3.40	8.71±2.48	0.0022±0.2446	
	Ti-O	0.61±0.17	1.90±3.20	8.71±2.48	0.0008±0.0012	
	Ti-O	1.22±0.34	2.06±0.12	8.71±2.48	0.0035±0.0243	
	Ti-O	0.61±0.17	2.48±0.10	8.71±2.48	0.0055±0.0155	
	Ti-S / Ti-Ti	1.22±0.34	3.26±0.03	8.71±2.48	0.0019±0.0045	
	Ti-O-Ti	1.22±0.34	3.62±0.04	8.71±2.48	0.0007±0.0011	
	Ti-Ti	1.22±0.34	3.65±0.04	8.71±2.48	0.0200±0.0012	
$TiOSO_4$ powder						
	Ti-O	2.00	1.71±0.03	3.13±2.53	0.0007±0.0011	**A**
	Ti-O	4.00	1.93±0.02	3.13±2.53	0.0014±0.0021	**B**
	Ti-S	4.00	3.22±0.04	3.13±2.53	0.0111±0.0076	**C**
	Ti-O-S	4.00	3.50±0.04	3.13±2.53	0.0081±0.0174	**D**
	Ti-Ti	4.00	3.56±0.04	3.13±2.53	0.0007±0.0012	**E**
	Ti-O-Ti	8.00	3.58±0.04	3.13±2.53	0.0052±0.0037	
	Ti-O-Ti	4.00	3.59±0.04	3.13±2.53	0.0018±0.0023	
{Ti_{18}} powder						
	Ti-O	1.00	1.66±0.03	-0.67±3.05	0.0006±0.0011	**1**
	Ti-O	1.00	1.83±0.03	-0.67±3.05	0.0024±0.0070	**2**
	Ti-O	1.00	1.86±0.03	-0.67±3.05	0.0045±0.0092	
	Ti-O	2.00	1.96±0.04	-0.67±3.05	0.0200±0.0012	**3**
	Ti-O	1.00	1.98±0.05	-0.67±3.05	0.0200±0.0008	
	Ti-S / Ti-Ti	2.00	3.25±0.03	10.5±2.1	0.0007±0.0011	**4**
	Ti-O-Ti	2.00	3.62±0.03	10.5±2.1	0.0019±0.0036	**5**

[1] *The coordination number (CN) for the {Ti_{18}} and $TiOSO_4$ solid samples is set to the ideal coordination number in the crystalline lattice, and the CN in the solution samples are normalized to this value.*

Crystallography

Table S2 Crystal data and structure refinement for the obtained $\{Ti_{18}\}$-cluster.

Moiety formula	$[Ti_{18}O_{27}(H_2O)_{25}(SO_4)9.5](Cl)_{5.5}(TBA)_6 \cdot 13.5H_2O$
Empirical formula	$C_{190}H_{412}Cl_{10}N_{12}O_{207.66}S_{19}Ti_{36}$
Formula weight	8875.89
Temperature/K	173.15
Crystal system	monoclinic
Space group	$P2_1$
a/Å	18.2006(7)
b/Å	17.8315(7)
c/Å	30.6879(14)
α/°	90
β/°	91.136(2)
γ/°	90
Volume/Å^3	9957.6(7)
Z	1
ρ_{calc}g/cm^3	1.479
μ/mm^{-1}	8.152
F(000)	4163.0
Crystal size/mm^3	0.08 × 0.04 × 0.02
Radiation	CuKα (λ = 1.54178)
2Θ range for data collection/°	4.856 to 99.808
Index ranges	$-17 \leq h \leq 18, -17 \leq k \leq 17, -30 \leq l \leq 30$
Reflections collected	50933
Independent reflections	19697 [R_{int} = 0.0749, R_{sigma} = 0.1049]
Data/restraints/parameters	19697/3/1989
Goodness-of-fit on F^2	1.021
Final R indexes [I>=2σ (I)]	R_1 = 0.0858, wR_2 = 0.2191
Final R indexes [all data]	R_1 = 0.1099, wR_2 = 0.2400
Largest diff. peak/hole / e Å^{-3}	1.06/-0.55
Flack parameter	0.111(6)

Table S3 Calculated parameters of the refinement for TiO_2 anatase nanoparticle.

I 41/a m d	R_{wp} = 45.25%*	reduced χ^2 = 0.0192
Atom	Occ	U_{iso}
Ti	1	0.01330
O	1	0.02475
a = b = 3.774 Å	c = 9.546 Å	d (diameter) = 19.56 Å

*: the relatively great number is due to the nanoparticle refinement, see ref [11].

Table S4 Extracted quantitative data† from aged 0.25 M and 1.0 M $TiOSO_4$ solutions. Size is represented in Å in terms of R_g, while the percentage represents the relative population.

	0.25 M $TiOSO_4$‡	**1.0 M $TiOSO_4$§**
Freshly prepared sample		
1st population	5.5 Å – 100 %	5.3 Å – 100 %
2nd population	N.A.	N.A.
Half-way to precipitation		
1st population	5.8 Å – 93.9 %	5.7 Å – 98. 8%
2nd population	10.6 Å – 6.1 %	10.0 Å – 1.2 %
At precipitation		
1st population	5.4 Å – 92.7 %	5.5 Å – 93.7 %
2nd population	10.8 Å – 7.3 %	10.0 Å – 6.3 %

† *Analyses to determine size and relative populations were carried out utilizing IRENA macros with IgorPro 6.3 (Wavemetrics) software.*[1]

‡*Preciptiates after 6 days of aging*

§*Preciptiates after 45 days of aging*

References

1 J. Ilavsky and P. R. Jemian, *J. Appl. Crystallogr.*, 2009, **42**, 347–353.

2 R. Zhang, P. Thiyagarajan and D. M. Tiede, *J. Appl. Crystallogr.*, 2000, **33**, 565–568.

3 D. M. Tiede, R. Zhang, L. X. Chen, L. Yu and J. S. Lindsey, *J. Am. Chem. Soc.*, 2004, **126**, 14054–14062.

4 P. Juhas, T. Davis, C. L. Farrow and S. J. L. Billinge, *J. Appl. Crystallogr.*, 2013, **46**, 560–566.

5 C. L. Farrow, P. Juhas, J. W. Liu, D. Bryndin, E. S. Božin, J. Bloch, T. Proffen and S. J. L. Billinge, *J. physics. Condens. matter*, 2007, **19**, 335219.

6 *SAINT Plus Version 8.34a, Bruker Anal. X-rays Syst. Madison, WI.*

7 G. M. Scheldrick, *SADABS, Bruker-Siemens area Detect. Absorpt. other Correct. Version 2008/1*, 2006.

8 G. M. Sheldrick, *Acta Crystallogr. Sect. A Found. Crystallogr.*, 2015, **71**, 3–8.

9 G. M. Sheldrick, *Acta Crystallogr. Sect. A Found. Crystallogr.*, 2008, **64**, 112–122.

10 O. V. Dolomanov, L. J. Bourhis, R. J. Gildea, J. A. K. Howard and H. Puschmann, *J. Appl. Crystallogr.*, 2009, **42**, 339–341.

11 H.-W. Wang, D. J. Wesolowski, T. E. Proffen, L. Vlcek, W. Wang, L. F. Allard, A. I. Kolesnikov, M. Feygenson, L. M. Anovitz and R. L. Paul, *J. Am. Chem. Soc.*, 2013, **135**, 6885–6895.